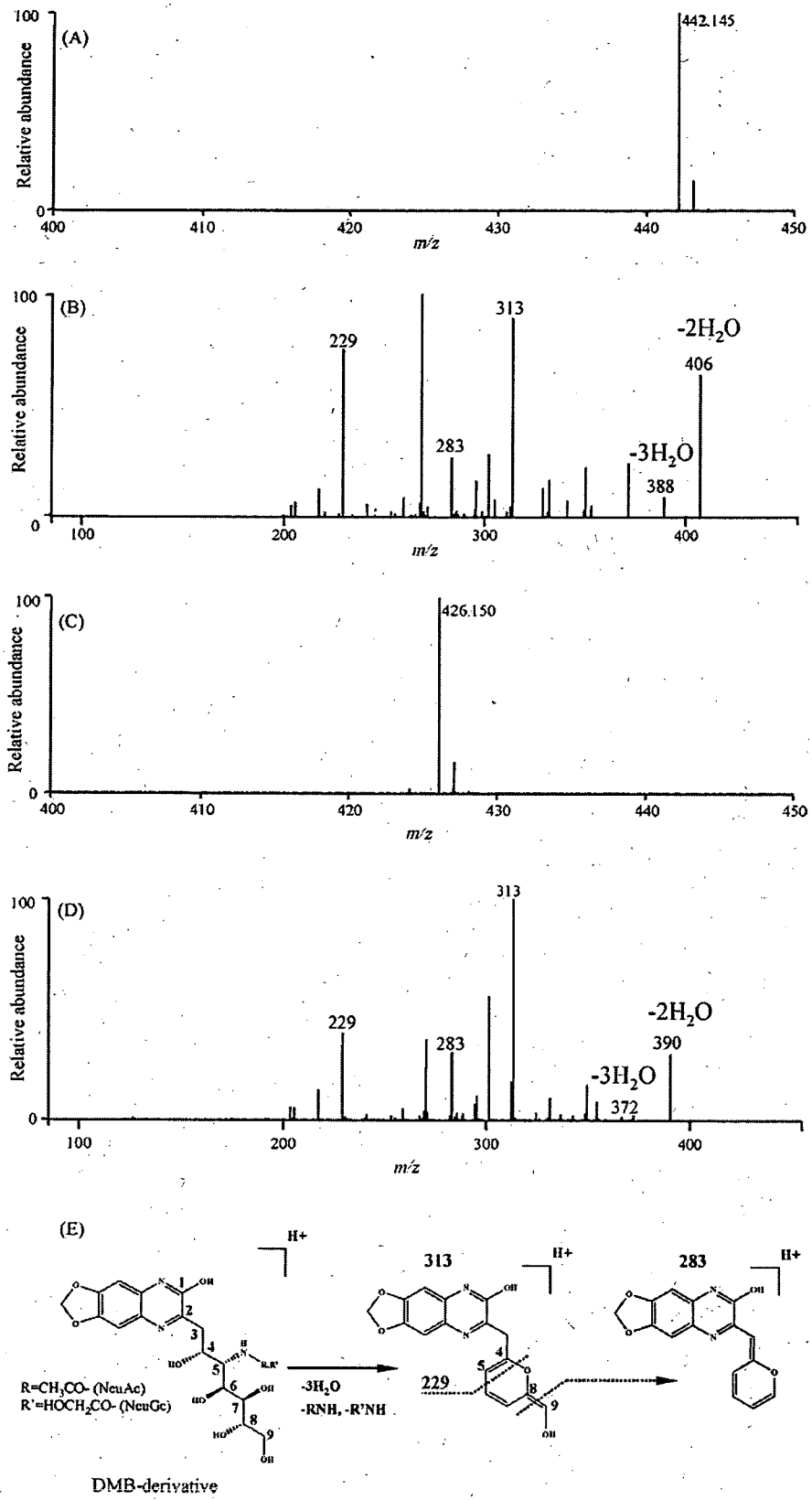

Fig. 2. (A) Typical MS spectrum of peak a. (B) MS/MS spectrum of $[M+H]^+$ (*m/z* 442.145) acquired from around peak a. (C) Typical MS spectrum of peak b. (D) MS/MS spectrum of $[M+H]^+$ (*m/z* 426.150) acquired from around peak b. (E) Fragmentation of DMB-NeuGc and DMB-NeuAc.

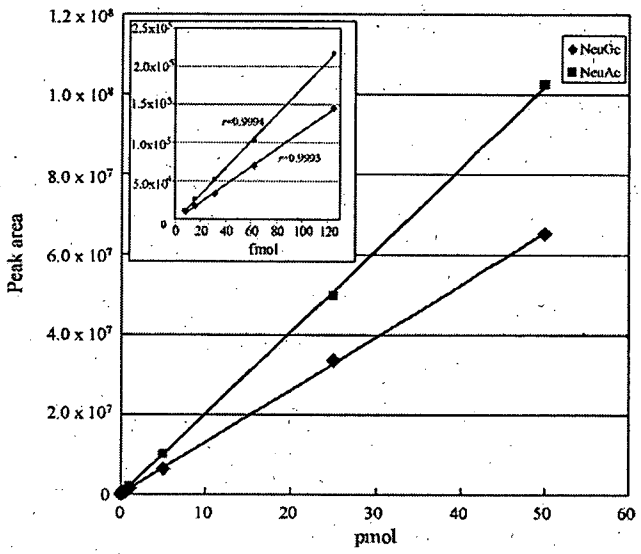

Fig. 3. Calibration curves of DMB-NeuGc ($r=0.9998$) and DMB-NeuAc ($r=0.9995$).

tonitrile (pump A) and 0.1% formic acid/80% acetonitrile (pump B) with a linear gradient of 10–90% of B in 30 min at a flow rate of 750 nl/min. On-line MS and MS/MS were performed using an Fourier transformation ion cyclotron resonance (FT)/ion trap (IT) type mass spectrometer (LTQ-FT, Thermo-Electron, San Jose, CA, USA) equipped with a nanoelectrospray ion source (AMR, Tokyo, Japan). DMB-NeuAc and DMB-NeuGc were determined by selected ion monitoring (SIM) in the positive ion mode. The analytical conditions were set to 200 °C for capillary temperature, 1800 eV spray voltage, *m/z* 400–450 scan range, and 35% collision energy. The automatic gain control (AGC) value, which is adjusted for the amount of imported ions for FTMS, was set to 5×10^4. Maximum injection times, which are the adjusted times of imported ions, for ITMS and FTMS, were set to 50 and 1250 ms, respectively.

2.6. Method validation

The linearity of the signal intensity peak area of DMB-NeuAc and DMB-NeuGc was assessed by injections of 0.0078–500 pmol DMB derivatives. Correlation coefficients were calibrated using a least-squares linear regression model. The detection limit (DL) and the quantification limit (QL) were calculated using the formulas $DL = 3.3 \times \sigma/\text{slope}$ (σ: average of noise on chromatograph) and $QL = 10 \times \sigma/\text{slope}$, respectively. Accuracy and precision were determined by measuring three samples, where NeuGc spiked at the concentration of 50 fmol to the membrane fraction of cells cultured in serum-free medium which contains no NeuGc before the derivatization of NeuGc with DMB. Accuracy was calculated by comparison of the mean peak area and the calibration curve. Precision was estimated by relative standard deviation (RSD) from three samples.

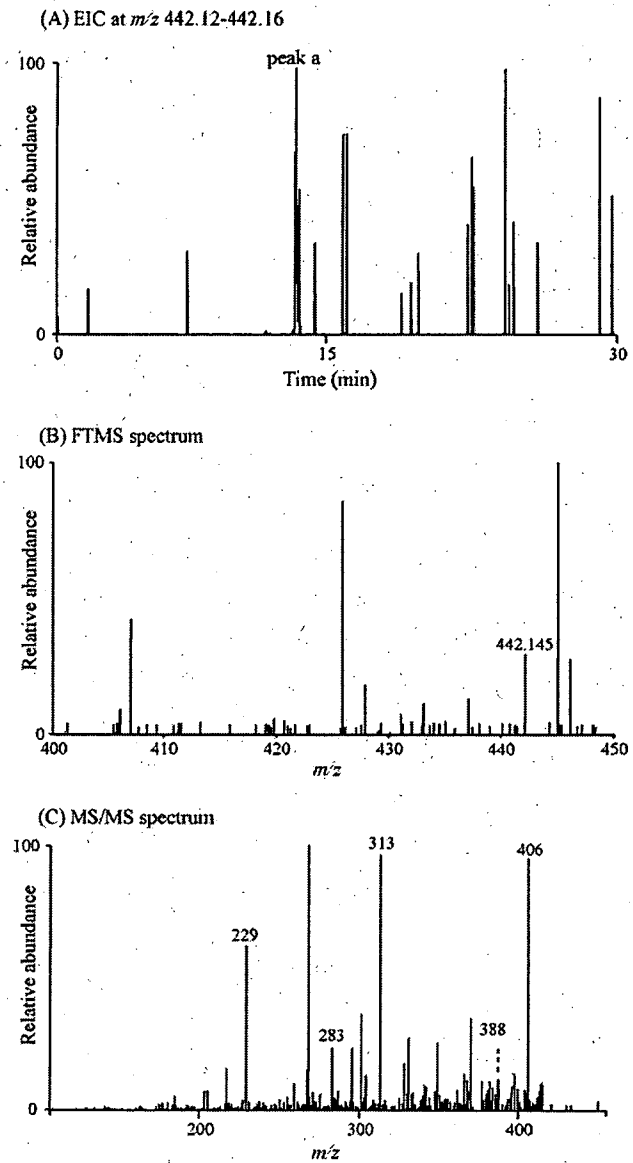

Fig. 4. Detection of DMB-NeuGc in the membrane fractions of HL-60RG cells (2.5×10^3) cultured with 10% FCS. (A) EIC at *m/z* 442.12–442.16 obtained by SIM. (B) Typical MS spectrum of peak a. (C) MS/MS spectrum of $[M+H]^+$ (*m/z* 442.145) acquired from around peak a.

3. Results and discussion

3.1. Analysis of NeuGc and NeuAc by nanoLC/FTMS

It was reported that DMB-NeuGc yielded its dehydrated ion (*m/z* 424) together with molecular ion (*m/z* 442) by MS in the positive ion mode [18,21]. To control the dehydration of molecular ion in the ion trap device, AGC value, which regulates the amount of ions trapped into ion trap device, was set to 5×10^4 (default value, 5×10^5). This value was also useful for the detection of molecular ion of DMB-NeuAc.

Using the AGC value at 5×10^4, SIM (*m/z* 400–450) was carried out in the positive ion mode. When a mix-

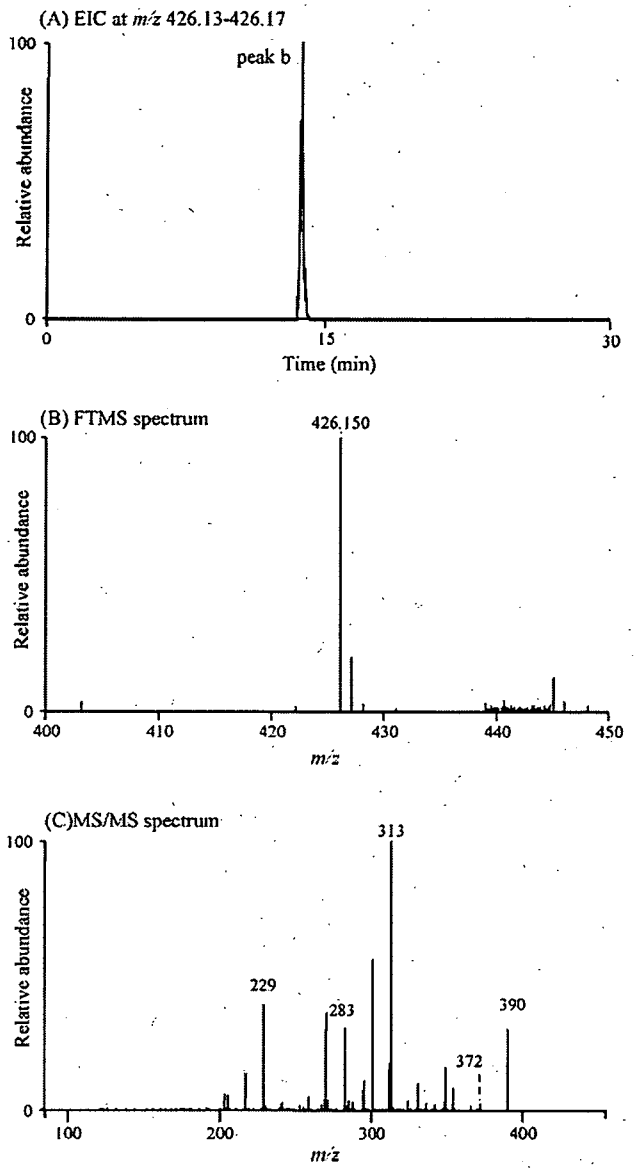

Fig. 5. Detection of DMB-NeuAc in the membrane fractions of HL-60RG cells (2.5×10^3) cultured with 10% FCS. (A) EIC at *m/z* 426.13–426.17 obtained by SIM. (B) Typical MS spectrum of peak b, (C) MS/MS spectrum of $[M+H]^+$ (*m/z* 426.150) acquired from around peak b.

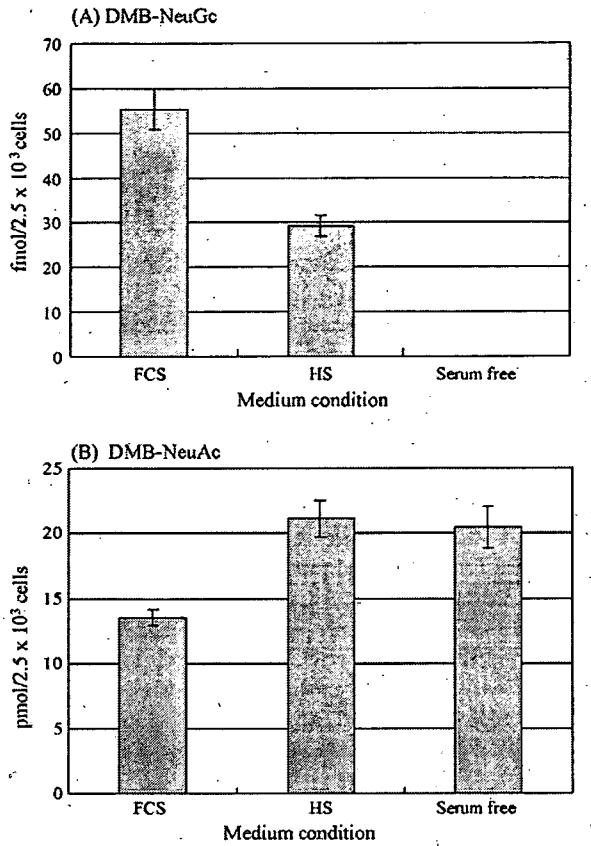

Fig. 6. Levels of (A) NeuGc and (B) NeuAc in the membrane fraction of HL-60RG cells (2.5×10^3) cultured with 10% FCS, 10% human serum (HS) and serum-free medium. Values are the means ± SD ($n = 3$).

ture of DMB-NeuGc and DMB-NeuAc (2 pmol each) was subjected to nanoLC/MS, two peaks appeared at 14 min (peak a) and 15 min (peak b) on the extracted ion chromatogram (EIC) at *m/z* 426.13–426.17 and *m/z* 442.12–442.16 (Fig. 1).

As shown in Fig. 2A, the *m/z* values of molecular ions around 14 min (*m/z* 442.145) suggest the elution of DMB-NeuGc in peak a. The structure of the DMB derivative at peak a was confirmed by the product ion spectra acquired from $[M+H]^+$ (*m/z* 442.145) as a precursor ion (Fig. 2B). Product ions missing two and three molecules of H_2O were found at *m/z* 406 and 388 in MS/MS spectra. Ions losing three H_2O and glycolyl groups (*m/z* 313), cross-ring fragment ion (*m/z* 229) and fragment ion yielded by loss of formaldehyde (*m/z* 283) were also formed by MS/MS (Fig. 2E). The fragment pattern of the MS/MS spectrum from $[M+H]^+$ (*m/z* 442.145) was consistent with that of DMB-NeuGc in the previous report [21]. Fragments at *m/z* 406 and 388 are DMB-NeuGc characteristic ions, which could be used for specific determination of DMB-NeuGc. Likewise, peak b was identified as DMB-NeuAc by molecular ions (*m/z* 426.150) and their product ions (*m/z* 390, 372, 313, 283 and 229) formed by MS/MS of $[M+H]^+$ (*m/z* 426.150) as a precursor ion (Fig. 2C and D).

Calibration curves were prepared by the injection of DMB-NeuGc and DMB-NeuAc from 0.0078 to 500 pmol. The linearity of DMB-NeuGc and DMB-NeuAc was confirmed in the range of 0.0078–50 pmol with the regression equations of $Y = 1.31 \times 10^6 X - 9028.5$ ($r = 0.9998$) and $Y = 2.03 \times 10^6 X - 21548.0$ ($r = 0.9995$), respectively (Fig. 3). DL and QL of DMB-NeuGc were 8.6 and 26.3 fmol, and those of DMB-NeuAc were 5.6 and 16.9 fmol, respectively. The use of FT/MS gave an accuracy of 92.4% by eliminating contaminants by using accurate *m/z* values. The precision of this method for NeuGc was 7.3%. Compared to the former method, in which a micro or semi-micro column and the quadrupole mass spectrometer were used for the detection of picomole levels of DMB derivatives, SIM by using nanoLC/FTMS achieved the specific detection of DMB-derivatized sialic acids at a lower level. The

method using nanoLC/FTMS and nanoLC/MS/MS allows not only the determination of DMB-derivatives with similar sensitivity as the fluorescence detection but also the identification of sialic acid species.

3.2. Quantification of NeuAc and NeuGc in membrane fraction of HL-60RG cells

Using HL-60RG cells as model cells, the potential of this method for the quantification of NeuGc on the cell membrane was evaluated. The membrane fraction from cells (1×10^6) cultured with 10% FCS was prepared by ultracentrifugation. Sialic acids were released by treatment with 2 M acetic acid at 80 °C for 3 h and derivatized with DMB. DMB derivatives (2.5×10^3 cells) were subjected to nanoLC/MS and nanoLC/MS/MS in SIM mode. As shown in Fig. 4A, some peaks appeared in EIC at *m/z* 442.12–442.16. Based on the retention time as well as the *m/z* value of molecular ion (*m/z* 442.145), peak a that appeared at 14 min was assigned to be a peak of NeuGc (Fig. 4B). Fig. 4C shows the MS/MS spectrum acquired from $[M+H]^+$ (*m/z* 442.145) as precursor. The NeuGc-characteristic ions at *m/z* 406 and 388 together with other product ions at *m/z* 313, 283 and 229 clearly indicate the presence of NeuGc in the membrane fraction of HL-60RG cells. In the EIC at *m/z* 426.13–426.17, the single peak was observed at 15 min (Fig. 5A). The molecular ion at *m/z* 426.150, and product ions at *m/z* 390, 372, 313, 283 and 229 acquired at 15.13 min suggest that DMB-NeuAc is eluted in peak b (Fig. 5B and C). The levels of NeuGc and NeuAc in the membrane fraction from HL-60RG cells (2.5×10^3 cells) cultured with 10% FCS were 55.4 ± 4.6 fmol and 13.5 ± 0.6 pmol, respectively (Fig. 6)

After the cultivation of HL-60RG cells with human serum for 10 days (medium was changed four times), NeuGc and NeuAc were determined by the proposed method. Fig. 7A shows the EIC at *m/z* 442.12–442.16 obtained by nanoLC/MS. In spite of cultivation in human serum, an obvious peak still appeared at 14 min. Molecular ion (*m/z* 442.145) and NeuGc-characteristic product ions found in the MS/MS spectrum acquired from the molecular ion clearly indicate the presence of NeuGc in the membrane fraction (Fig. 7B and C). The levels of NeuGc and NeuAc in cells (2.5×10^3) cultured in 10% human serum were 29.2 ± 2.4 fmol and 21.0 ± 1.4 pmol, respectively (Fig. 6).

In contrast, no significant peaks appeared in EIC at *m/z* 442.12–442.16 when HL-60RG cells were cultured in serum-free medium for 14 days (medium was changed four times). The level of NeuAc in cells cultured in serum-free medium was 20.5 ± 1.6 pmol (Fig. 6).

As shown in Figs. 4A and 7A, there are many different molecules detected at *m/z* 442.14–442.16 in the cells, which makes it difficult to determine a small amount of NeuGc in the membrane fraction by the low-resolution mass spectrometry. The DMB-NeuGc-specific detection was achieved by acquisition of both the accurate mass by FTMS and the characteristic product ions arisen from DMB-NeuGc by MS/MS.

Our method needs only 2.5×10^3 cells for one injection and is applicable to the determination of NeuGc in cell therapy products. The incorporation of dietary NeuGc into human serum has been reported by Tangvoranuntalul et al. [23], which has raised concerns about NeuGc contamination of cell therapy products through cultivation with human serum. Although using our method, we demonstrated the existence of NeuGc in human cells cultured with human serum, NeuGc could not be detected in human cells cultured in serum-free medium in which no NeuGc exists. These results suggest the difficulty of avoiding NeuGc contamination of cell therapy products during the manufacturing process. Further study to assess the immunogenicity of incorporated NeuGc is necessary to ensure the safety and efficacy of cell therapy products, and our method is useful for the sensitive and quantitative analysis of NeuGc in cell therapy products.

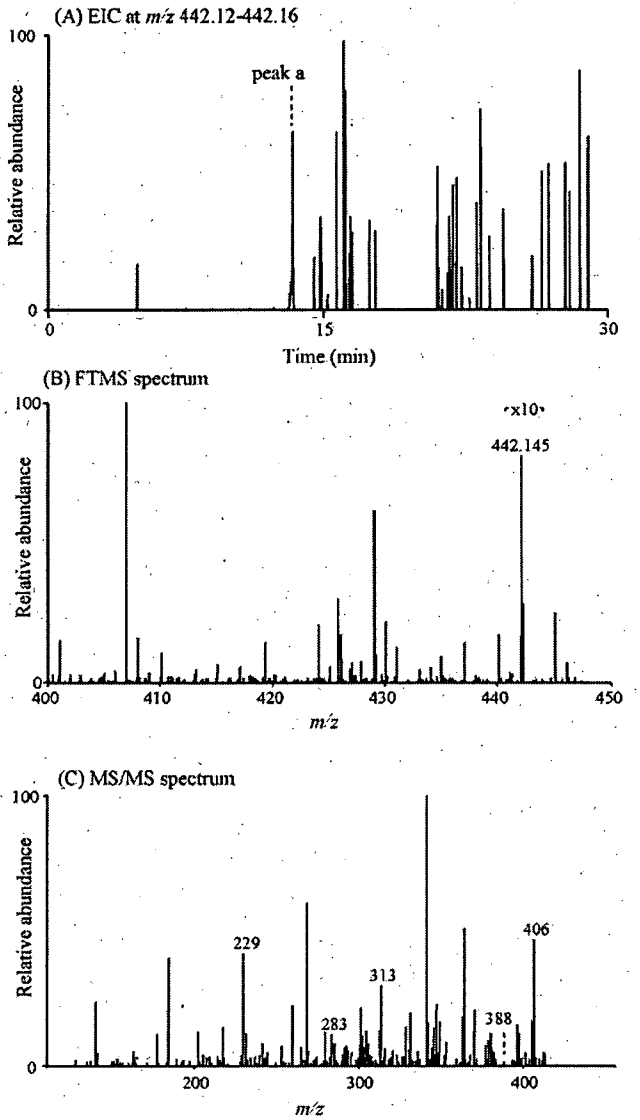

Fig. 7. Detection of DMB-NeuGc in the membrane fractions of HL-60RG cells (2.5×10^3) cultured with 10% human serum. (A) EIC at *m/z* 442.12–442.16 obtained by SIM. (B) Typical MS spectrum of peak a. (C) MS/MS spectrum of $[M+H]^+$ (*m/z* 442.145) acquired from around peak a.

Acknowledgements

This study was supported in part by a Grant-in-Aid from the Ministry of Health Labor and Welfare, and Core Research for the Evolutional Science and Technology Program, Japan Science and Technology Corp.

References

[1] C. Traving, R. Schauer, Cell Mol. Life Sci. 54 (1998) 1330.
[2] T. Angata, A. Varki, Chem. Rev. 102 (2002) 439.
[3] A. Varki, Glycobiology 2 (1992) 25.
[4] R. Schauer, Adv. Carbohydr. Chem. Biochem. 40 (1982) 131.
[5] S. Kitazume, K. Kitajima, S. Inoue, S.M. Haslam, H.R. Morris, A. Dell, W.J. Lennarz, Y. Inoue, J. Biol. Chem. 271 (1996) 6694.
[6] R. Schauer, J. Haverkamp, M. Wember, J.P. Kamerling, J.F. Vliegenthart, Eur. J. Biochem. 62 (1976) 237.
[7] N. Kawasaki, S. Itoh, M. Ohta, T. Hayakawa, Anal. Biochem. 316 (2003) 15.
[8] M. Nakano, K. Kakehi, M.H. Tsai, Y.C. Lee, Glycobiology 14 (2004) 431.
[9] E.A. Muchmore, S. Diaz, A. Varki, Am. J. Phys. Anthropol. 107 (1998) 187.
[10] A. Irie, S. Koyama, Y. Kozutsumi, T. Kawasaki, A. Suzuki, J. Biol. Chem. 273 (1998) 15866.
[11] H.H. Chou, H. Takematsu, S. Diaz, J. Iber, E. Nickerson, K.L. Wright, E.A. Muchmore, D.L. Nelson, S.T. Warren, A. Varki, Proc. Natl. Acad. Sci. U. S. A. 95 (1998) 11751.
[12] H. Higashi, M. Naiki, S. Matuo, K. Okouchi, Biochem. Biophys. Res. Commun. 79 (1977) 388.
[13] J.M. Merrick, K. Zadarlik, F. Milgrom, Int. Arch. Allergy Appl. Immunol. 57 (1978) 477.
[14] M.J. Martin, A. Muotri, F. Gage, A. Varki, Nat. Med. 11 (2005) 228.
[15] A. Heiskanen, T. Satomaa, S. Tiitinen, A. Laitinen, S. Mannelin, U. Impola, M. Mikkola, C. Olsson, H. Miller-Podraza, M. Blomqvist, A. Olonen, H. Salo, P. Lehenkari, T. Tuuri, T. Otonkoski, J. Natunen, J. Saarinen, J. Laine, Stem Cells 25 (2007) 197.
[16] A.E. Manzi, S. Diaz, A. Varki, Anal. Biochem. 188 (1990) 20.
[17] S. Hara, M. Yamaguchi, Y. Takemori, K. Furuhata, H. Ogura, M. Nakamura, Anal. Biochem. 179 (1989) 162.
[18] M. Bardor, D.H. Nguyen, S. Diaz, A. Varki, J. Biol. Chem. 280 (2005) 4228.
[19] M. Ito, K. Ikeda, Y. Suzuki, K. Tanaka, M. Saito, Anal. Biochem. 300 (2002) 260.
[20] F.N. Lamari, N.K. Karamanos, J. Chromatogr. B 781 (2002) 3.
[21] A. Klein, S. Diaz, I. Ferreira, G. Lamblin, P. Roussel, A.E. Manzi, Glycobiology 7 (1997) 421.
[22] H.H. Chou, T. Hayakawa, S. Diaz, M. Krings, E. Indriati, M. Leakey, S. Paabo, Y. Satta, N. Takahata, A. Varki, Proc. Natl. Acad. Sci. U. S. A. 99 (2002) 11736.
[23] P. Tangvoranuntakul, P. Gagneux, S. Diaz, M. Bardor, N. Varki, A. Varki, E. Muchmore, Proc. Natl. Acad. Sci. U. S. A. 100 (2003) 12045.

Progress in Hematology

International Journal of
HEMATOLOGY

Ways for a Mesenchymal Stem Cell to Live on Its Own: Maintaining an Undifferentiated State Ex Vivo

Masashi Toyoda, Hidekazu Takahashi, Akihiro Umezawa

Department of Reproductive Biology, National Institute for Child Health and Development, Tokyo, Japan

Received April 3, 2007; accepted May 2, 2007

Abstract

Like all stem cells, mesenchymal stem cells (MSC) must balance self-renewal and differentiation. Complex regulatory mechanisms are required to keep stem cells in an undifferentiated, self-renewing state and to mediate their subsequent differentiation and proliferation. In this review, we discuss how adequate numbers of MSC can be maintained in culture. In particular, we focus on identification of the cell culture conditions needed to maintain general, nonspecific potential as a stem cell over time and through replication. It would be extremely advantageous to be able to maintain MSC populations in a completely undifferentiated state and to determine and switch on specific differentiation as and when required.
Int J Hematol. 2007;86:1-4. doi: 10.1532/IJH97.07055

Key words: Mesenchymal stem cells; Cell culture; Differentiation; Cell growth; Senescence

1. Introduction

Mesenchymal stem cells (MSC) are attracting a great deal of attention, because they represent a valuable source of cells for use in regenerative medicine [1]. Use of MSC entails no ethical or immunologic problems, and they provide an excellent model of cell differentiation in biology. Not surprisingly, mesenchymal cell biology is a complex and rapidly evolving field. Critical unanswered questions remain: What defines an MSC (as opposed to just a mesenchymal cell), and what provides MSC with their unique properties?

Stem cell biology is based on the principle that any tissue may contain cells that possess the potential for both self-renewal and differentiation into one or more cell types. Mesenchymal cells are derived from an organ's supporting tissue, as opposed to parenchyma or the supporting framework of an animal organ, which typically consists of connective tissue. Among these cells exist stem cells, which have two basic processes, ie, self-renewal and differentiation. MSC were first discovered in 1976 by Friedenstein, who described clonal, plastic-adherent cells from bone marrow that provided a physical scaffold for hematopoiesis and that could differentiate into osteoblasts, chondrocytes, and adipocytes in vitro [2]. To date, investigators have demonstrated that MSC per se can be recovered from a variety of adult tissues and have the capacity to differentiate into a variety of specific cell types [3-8]. The mesenchymal phenotype can be maintained under optimal culture conditions, and MSC in vitro are recognized as adherent fibroblastic cells with a generally spindle shape, although some candidate populations of cells are more spherical with few spindle-shaped cells [9]. This heterogeneous population is too "crude" to consist solely of MSC. Although MSC can be harvested from a variety of tissues and have multipotency (ie, the capability to differentiate into numerous tissue lineages, including myoblasts, cardiomyocytes, osteoblasts, adipocytes, chondrocytes, and possibly even neural cells), MSC populations cannot easily be induced to differentiate into one lineage at the same time. There are some cell populations that behave like progenitor cells with monopotency or bipotency. In this review, we describe how MSC derived from a variety of tissues have tissue-specific characteristics and discuss optimal culture conditions that can allow the cells both to keep proliferating in an undifferentiated, self-renewing state and to permit mediation of their future differentiation.

Correspondence and reprint requests: Akihiro Umezawa, Department of Reproductive Biology, National Institute for Child Health and Development, 2-10-1, Okura, Setagaya-ku, Tokyo, 157-8535, Japan; 81-3-5494-7047
(e-mail: umezawa@1985.jukuin.keio.ac.jp).

2. MSC Optimally Require Their Original Milieu

Stem cells are indispensable entities in most multicellular organisms in that they are responsible for forming tissues during early development and for maintaining them in the adult stage. Because all somatic stem cells, including MSC, have the same genetic material, every cell type has the potential to express a stem cell phenotype under specific conditions; that is, tissue-specific flexibility is inherent. Mesenchymal cells, of which connective tissue is mainly composed, do not develop into a tissue or an organ. The cells synthesize the extracellular matrix by themselves and in vitro establish favorable environments for growth. Mesenchymal cell cultures can be made from suspensions of cells dissociated from tissues, and microscopical and biochemical analyses facilitate exploration of the effects of adding or removing specific molecules, such as hormones or growth factors.

Cells vary in their needs in a cell type–specific manner, and cells can therefore be categorized or defined by their requirements. Bone marrow–derived MSC, for example, can be compared with umbilical cord blood–derived MSC. Several methods are available for distinguishing between these two types of cells. One such method is flow cytometric analysis of markers that appear on the surfaces of the cells. Some surface marker characteristics of bone marrow–derived MSC are the same as those of cord blood–derived MSC (eg, $CD29^+$, $CD44^+$, $CD55^+$, $CD59^+$, $CD34^-$, and $CD117^-$ [10-12]). On the other hand, the CD90 and CD133 markers can be used to distinguish cord blood–derived cells from bone marrow–derived cells, because these markers are expressed in multipotent marrow-derived cells but not in cord blood–derived cells [12]. As yet, no surface markers have been identified that define MSC. Another method is complementary DNA microarray/chip technology. Because of the logical connection between gene expression and cell function, gene expression patterns can predict the variation in cell phenotypes and reveal novel phenotypic aspects of the cells and tissues studied. In mesenchymal cell culture, expression of genes encoding growth factor receptors is an important factor in microarray analysis–based investigations of the effects of growth factors, because cells dissociated from different tissues, such as bone marrow and cord blood, have different responses to growth factors (Table 1). This response affects differentiation potential. Bone marrow–derived cells can differentiate into osteoblasts, chondrocytes, cardiomyocytes, adipocytes, skeletal myocytes, and neural cells and do so according to the specific cell culture conditions, whereas cord blood–derived cells exhibit only osteogenic and adipogenic potential under the same conditions.

How can the microenvironment, culture conditions, or growth factors dictate the identity of MSC and their production of different progeny? Serum plays a critical role in the growth of cells in vitro by providing components such as amino acids, lipids, growth factors, vitamins, hormones, and attachment factors, by acting as a pH buffer, and by providing protease inhibitors. Most media for mesenchymal cell culture include a poorly defined mixture of macromolecules in the form of fetal calf serum; however, the use of serum for MSC culture makes it difficult to know which specific macromolecules a particular type of cell requires for survival and normal function. This difficulty led to the development of serum-free chemically defined media. In addition to the usual molecules, such specialized media will need to contain essential growth factors that the MSC require in culture. The primary requirements of MSC in culture reflect the origin of the cells; that is, investigators have to try to recreate the specific native tissue/organ milieu of the cells' origin. Identification of a means to create an "Elysium" or ideal stress-free native environments for cultivating and maintaining MSC will bestow significant benefits for future stem cell therapeutics.

3. The Paradox of Cell Growth versus Life Span

In cell culture it is important not only to remove animal serum from the culture medium (for reasons of medical safety with respect to infectious diseases [13-15]) but also to obtain large numbers of cells for use in therapy. Cells must be propagated in vitro to obtain the large numbers needed for biomedical procedures; however, Hayflick's problem is unavoidable in normal cells [16,17]. Most vertebrate cells stop dividing after a finite number of divisions in culture, a process called *senescence* [17,18]. Senescence is classified into two categories: "stress-induced premature senescence" (or "telomere-independent senescence") and "replicative senescence" (or "telomere-dependent senescence") [19-21]. Marrow-derived mesenchymal cells divide approximately 25 to 40 times [11,22] in culture before they cease dividing or reach senescence (M0, mortality stage 0; ie, premature senescence), whereas a few cells that overcome this step restart proliferation but stop dividing again in replicative senescence (M1) (Figure 1).

To resolve these problems, investigators can extend the life span of bone marrow–derived MSC via retroviral transduction of human telomerase reverse transcriptase (hTERT) and human papillomavirus type 16 E6 and/or E7 genes [11]. A significant observation is that an increase in telomerase

Table 1.
Reactivities of Mesenchymal Stem Cells to Growth Factors*

	MSC	UCB	UE6E7T-12	UE7T-13
PDGF	+++	+++	+++	+++
EGF	+++	++	+++	++
aFGF	+++	++	++	+
bFGF	+++	+++	+++	++
LIF	–	+	++	+
VEGF	+	+	+	–
HGF	–	–	+	–
IGF-1	+	+	–	–
IL-1	–	–	–	++
IL-6	–	–	+	–

*Plus and minus symbols show the strength of growth factor reactivity based on cell proliferation. MSC indicates human bone marrow–derived mesenchymal stem cells; UCB, human umbilical cord blood–derived mesenchymal stem cells; UE6E7T-12 and UE7T-13, MSC transduced with human papillomavirus type 16 E6 and/or E7, and human telomerase reverse transcriptase (hTERT); PDGF, platelet-derived growth factor; EGF, epidermal growth factor; aFGF, acidic fibroblast growth factor; bFGF, basic FGF; LIF, leukemia inhibitory factor; VEGF, vascular endothelial growth factor; IGF-1, insulin-like growth factor 1; IL-1, interleukin 1.

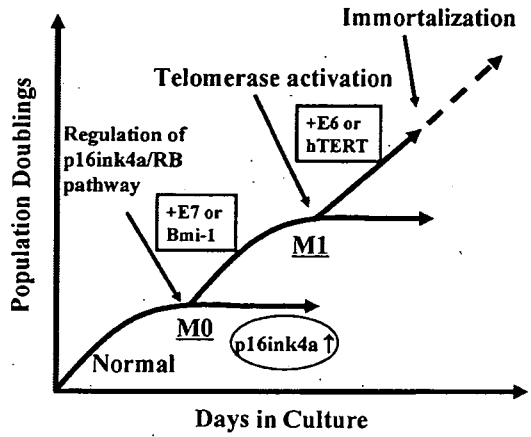

Figure 1. Life span of mesenchymal stem cells. Marrow-derived mesenchymal cells divide approximately 25 to 40 times in culture before they cease dividing or reach senescence (M0, mortality stage 0, ie, premature senescence). Some cells that overcome this step restart proliferation but stop dividing again in replicative senescence (M1). The system in which the p16ink4a/RB pathway is inhibited and telomerase is activated via transduction of *bmi-1*, human papillomavirus type 16 E6, E7, and hTERT is efficient in extending cellular life span.

activity produced via hTERT induction is insufficient to prolong the life span of bone marrow–derived MSC [23], because p16ink4a, a cyclin-dependent kinase inhibitor, is up-regulated [22]. This up-regulation of p16ink4a is directly linked to an increase in the number of cell doublings [24]. Inhibition of the p16/Rb pathway is sufficient to prolong the life span of cells in cultures of marrow-derived cells [11,22]. The p16ink4a/RB braking pathway leading to senescence can be inhibited by inducing the human papillomavirus type 16 E7 gene and/or *bmi-1*. *bmi-1*, one of the polycomb-group genes, has been used to inhibit p16ink4a transcription in order to prolong life span [25,26]. In addition, induction of the human papillomavirus type 16 E6 gene, which inhibits the p53 pathway, allows long-term cultivation of these cells. This system, in which the p16ink4a/RB pathway is inhibited and telomerase is activated, is highly efficient in extending the life span of bone marrow–derived MSC [23]. The life span of cord blood–derived MSC can be extended with hTERT alone [12].

Cell characteristics remain unaffected by *bmi-1*, E6, E7, and hTERT. The surface markers and the growth factor reactivities of transduced cells are unchanged (Table 1), and the transduced cells maintain their capabilities as stem cells [12,22]. So, can multipotent MSC with an extended life span be made available for cell-based therapy? It appears that transduced cells do not transform according to classic criteria: they do not generate a tumor in immunosuppressed interleukin 2 receptor knock-out NOD-SCID mice [22], they do not form foci in vitro, and they stop dividing after confluence. We cannot rule out the possibility, however, that gene-transduced bone marrow cells will become tumorigenic in patients several decades after commencement of cell therapy. What must be taken into account is that even when nononcogenic genes are introduced for cell-based therapy to increase cell growth and prolong life span, cases of leukemia have occurred in severe combined-immunodeficient patients treated with gene-modified lymphocytes [27]. Because of these failures, more time will be required before gene-modified cells can be used for regenerative medicine. Alleviation of culture stress is thus necessary to prolong the life span of mesenchymal cells.

Signaling from growth factor receptors caused by exogenously added growth factors induces p16ink4a protein through p38 and should selectively inhibit the prolongation of the cell life span without affecting growth factor–dependent cell proliferation through the classic Mek-Erk MAPK pathway (Figure 2A). Excessive stimulation by growth factors can be a cell senescence inducer, like oxidative stress and "culture shock" [28,29]. Growth factor–dependent acceleration of premature senescence or growth arrest is rather unexpected and unfavorable and is analogous to pressing down on the gas and brake pedals simultaneously [30,31]. Up-regulation of cell growth without affecting the cell life span, a key future goal of any cell-based therapy, would thus be a trade-off and create a fundamental quandary (Figures 2B and 2C).

4. Conclusion

Mammalian aging is associated with reduced regenerative capacity in tissues that contain stem cells. The aging process has been proposed to be at least partially caused by the senescence of progenitors with age; however, whether genes associated with senescence functionally contribute to physiological declines in progenitor activity has not yet been tested. Quantitative and qualitative changes do occur in stem cell populations with age [32-36]. The transition of multipotent stem cells to a more specific differentiated state is associated with simultaneous activation or inactivation of specific genes, and the promiscuous expression of many lineage-specific genes in primitive stem cells gradually decreases as cells reach a more mature state. Covalent modification

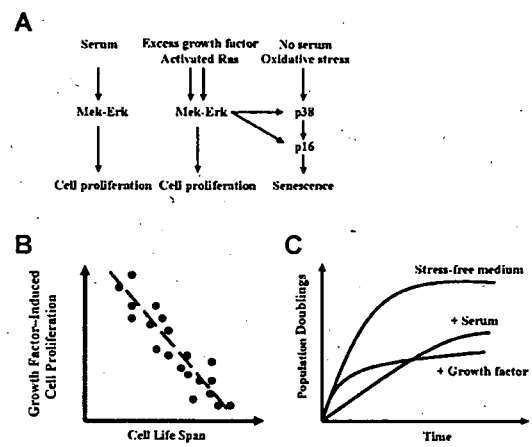

Figure 2. Signaling cascade and growth curves of mesenchymal stem cells for cell therapy. A, Scheme of the signaling cascade induced by stimuli leading to cell proliferation and senescence. B, Cell proliferation and the life span of mesenchymal cells are inversely correlated. C, Idealized cell growth profile in a stress-free medium. An ideal medium will help promote cell growth without affecting cellular aging.

includes acetylation, methylation, phosphorylation, and ubiquitination [37], and epigenetic regulation plays important roles in regulating gene expression. Consequently, the aging process influences stem cell–specific gene transcription. MicroRNA have recently been reported to be engaged in this regulation [38]. The goal of developing a clinically suitable medium for proliferating mesenchymal cells without affecting multipotency ex vivo appears feasible (Figure 2C), and its achievement should be beneficial to patients requiring an autologous or allogeneic transplant.

References

1. Alhadlaq A, Mao JJ. Mesenchymal stem cells: isolation and therapeutics. *Stem Cells Dev*. 2004;13:436-448.
2. Friedenstein AJ. Precursor cells of mechanocytes. *Int Rev Cytol*. 1976;47:327-359.
3. Makino S, Fukuda K, Miyoshi S, et al. Cardiomyocytes can be generated from marrow stromal cells in vitro. *J Clin Invest*. 1999;103:697-705.
4. Umezawa A, Maruyama T, Segawa K, Shadduck RK, Waheed A, Hata J. Multipotent marrow stromal cell line is able to induce hematopoiesis in vivo. *J Cell Physiol*. 1992;151:197-205.
5. Owen M. Marrow stromal stem cells. *J Cell Sci Suppl*. 1988;10:63-76.
6. Jaiswal N, Haynesworth SE, Caplan AI, Bruder SP. Osteogenic differentiation of purified, culture-expanded human mesenchymal stem cells in vitro. *J Cell Biochem*. 1997;64:295-312.
7. Pittenger MF, Mackay AM, Beck SC, et al. Multilineage potential of adult human mesenchymal stem cells. *Science*. 1999;284:143-147.
8. Sekiya I, Larson BL, Vuoristo JT, Cui JG, Prockop DJ. Adipogenic differentiation of human adult stem cells from bone marrow stroma (MSCs). *J Bone Miner Res*. 2004;19:256-264.
9. Horwitz EM. Mesenchymal cells: a basic review. 2002. Available at: http://www.celltherapysociety.org/files/documents/2005_Information_Booklet_-_Mesenchymal.doc. Accessed May 8, 2007.
10. Lee OK, Kuo TK, Chen WM, Lee KD, Hsieh SL, Chen TH. Isolation of multipotent mesenchymal stem cells from umbilical cord blood. *Blood*. 2004;103:1669-1675.
11. Takeda Y, Mori T, Imabayashi H, et al. Can the life span of human marrow stromal cells be prolonged by bmi-1, E6, E7, and/or telomerase without affecting cardiomyogenic differentiation? *J Gene Med*. 2004;6:833-845.
12. Terai M, Uyama T, Sugiki T, Li XK, Umezawa A, Kiyono T. Immortalization of human fetal cells: the life span of umbilical cord blood-derived cells can be prolonged without manipulating $p16^{INK4a}$/RB braking pathway. *Mol Biol Cell*. 2005;16:1491-1499.
13. Lennon DP, Haynesworth SE, Young RG, Dennis JE, Caplan AI. A chemically defined medium supports in vitro proliferation and maintains the osteochondral potential of rat marrow-derived mesenchymal stem cells. *Exp Cell Res*. 1995;219:211-222.
14. Wiles MV, Johansson BM. Embryonic stem cell development in a chemically defined medium. *Exp Cell Res*. 1999;247:241-248.
15. Yao CL, Chu IM, Hsieh TB, Hwang SM. A systematic strategy to optimize ex vivo expansion medium for human hematopoietic stem cells derived from umbilical cord blood mononuclear cells. *Exp Hematol*. 2004;32:720-727.
16. Hayflick L, Moorhead PS. The serial cultivation of human diploid cell strains. *Exp Cell Res*. 1961;25:585-621.
17. Campisi J. From cells to organisms: can we learn about aging from cells in culture? *Exp Gerontol*. 2001;36:607-618.
18. Wei W, Sedivy JM. Differentiation between senescence (M1) and crisis (M2) in human fibroblast cultures. *Exp Cell Res*. 1999;253:519-522.
19. Allsopp RC, Vaziri H, Patterson C, et al. Telomere length predicts replicative capacity of human fibroblasts. *Proc Natl Acad Sci U S A*. 1992;89:10114-10118.
20. Wright WE, Shay JW. The two-stage mechanism controlling cellular senescence and immortalization. *Exp Gerontol*. 1992;27:383-389.
21. Bodnar AG, Ouellette M, Frolkis M, et al. Extension of life-span by introduction of telomerase into normal human cells. *Science*. 1998;279:349-352.
22. Mori T, Kiyono T, Imabayashi H, et al. Combination of hTERT and *bmi-1*, E6, or E7 induces prolongation of the life span of bone marrow stromal cells from an elderly donor without affecting their neurogenic potential. *Mol Cell Biol*. 2005;25:5183-5195.
23. Okamoto T, Aoyama T, Nakayama T, et al. Clonal heterogeneity in differentiation potential of immortalized human mesenchymal stem cells. *Biochem Biophys Res Commun*. 2002;295:354-361.
24. Alcorta DA, Xiong Y, Phelps D, Hannon G, Beach D, Barrett JC. Involvement of the cyclin-dependent kinase inhibitor p16 (INK4a) in replicative senescence of normal human fibroblasts. *Proc Natl Acad Sci U S A*. 1996;93:13742-13747.
25. Haga K, Ohno S, Yugawa T, et al. Efficient immortalization of primary human cells by $p16^{INK4a}$-specific short hairpin RNA or Bmi-1, combined with introduction of hTERT. *Cancer Sci*. 2007;98:147-154.
26. Kim RH, Kang MK, Shin KH, et al. Bmi-1 cooperates with human papillomavirus type 16 E6 to immortalize normal human oral keratinocytes. *Exp Cell Res*. 2007;313:462-472.
27. Hacein-Bey-Abina S, Von Kalle C, Schmidt M, et al. LMO2-associated clonal T cell proliferation in two patients after gene therapy for SCID-X1. *Science*. 2003;302:415-419.
28. Sherr CJ, DePinho RA. Cellular senescence: mitotic clock or culture shock? *Cell*. 2000;102:407-410.
29. Toussaint O, Medrano EE, von Zglinicki T. Cellular and molecular mechanisms of stress-induced premature senescence (SIPS) of human diploid fibroblasts and melanocytes. *Exp Gerontol*. 2000;35:927-945.
30. Ramirez RD, Morales CP, Herbert BS, et al. Putative telomere-independent mechanisms of replicative aging reflect inadequate growth conditions. *Genes Dev*. 2001;15:398-403.
31. Raucci A, Laplantine E, Mansukhani A, Basilico C. Activation of the ERK1/2 and p38 mitogen-activated protein kinase pathways mediates fibroblast growth factor-induced growth arrest of chondrocytes. *J Biol Chem*. 2004;279:1747-1756.
32. Morrison SJ, Wandycz AM, Akashi K, Globerson A, Weissman IL. The aging of hematopoietic stem cells. *Nat Med*. 1996;2:1011-1016.
33. Harrison DE, Zhong RK, Jordan CT, Lemischka IR, Astle CM. Relative to adult marrow, fetal liver repopulates nearly five times more effectively long-term than short-term. *Exp Hematol*. 1997;25:293-297.
34. Kim M, Moon HB, Spangrude GJ. Major age-related changes of mouse hematopoietic stem/progenitor cells. *Ann N Y Acad Sci*. 2003;996:195-208.
35. Henckaerts E, Langer JC, Snoeck HW. Quantitative genetic variation in the hematopoietic stem cell and progenitor cell compartment and in lifespan are closely linked at multiple loci in BXD recombinant inbred mice. *Blood*. 2004;104:374-379.
36. Liang Y, Van Zant G, Szilvassy SJ. Effects of aging on the homing and engraftment of murine hematopoietic stem and progenitor cells. *Blood*. 2005;106:1479-1487.
37. Bandyopadhyay D, Medrano EE. The emerging role of epigenetics in cellular and organismal aging. *Exp Gerontol*. 2003;38:1299-1307.
38. Oakley EJ, Van Zant G. Unraveling the complex regulation of stem cells: implications for aging and cancer. *Leukemia*. 2007;21:612-621.

Hepatology Research 2007; 37: 1068–1079 doi: 10.1111/j.1872-034X.2007.00162.x

Original Article

Hepatic differentiation of human bone marrow-derived UE7T-13 cells: Effects of cytokines and CCN family gene expression

Takashi Shimomura,[1] Yoko Yoshida,[1] Tomohiko Sakabe,[1] Kyoko Ishii,[1] Kazue Gonda,[1] Rie Murai,[1] Kazuko Takubo,[2] Hiroyuki Tsuchiya,[1] Yoshiko Hoshikawa,[1] Akihiro Kurimasa,[1] Ichiro Hisatome,[3] Taro Uyama,[4] Akihiro Umezawa[4] and Goshi Shiota[1]

[1]*Division of Molecular and Genetic Medicine, Department of Genetic Medicine and Regenerative Therapeutics, Graduate School of Medicine, Tottori University,* [2]*Division of Oral and Maxillofacial Biopathological Surgery, Department of Medicine of Sensory and Motor Organs, Faculty of Medicine, Tottori University,* [3]*Division of Regenerative Therapeutics, Graduate School of Medicine, Tottori University, Tottori, and* [4]*Department of Reproductive Biology and Pathology, National Research Institute for Child Health and Development, Tokyo, Japan*

Aim: Bone marrow-derived mesenchymal stem cells (MSC) are expected to be an excellent source of cells for transplantation. We aimed to study the culture conditions and involved genes to differentiate MSC into hepatocytes.

Methods: The culture conditions to induce the efficient differentiation of human bone marrow-derived UE7T-13 cells were examined using cytokines, hormones, 5-azacytidine and type IV collagen.

Results: We found that combination of acidic fibroblast growth factor (aFGF), basic fibroblast growth factor (bFGF) and hepatocyte growth factor (HGF) with type IV collagen coating induced hepatic differentiation of UE7T-13 cells at over 30% frequency, where expression of albumin mRNA was increased over 20-fold. The differentiated cells had functions of albumin production, glycogen synthesis and urea secretion as well as expressing hepatocyte-specific genes. In addition, these cells have binuclear and cuboidal morphology, which is a characteristic feature of hepatocytes. During hepatic differentiation, UE7T-13 cells showed depressed expression of *WISP1* and *WISP2* genes, members of the CCN family. Conversely, knockdown of *WISP1* or *WISP2* gene by siRNA stimulated hepatic differentiation. The effect of aFGF/bFGF/HGF/type IV collagen coating and WISP1-siRNA on hepatic differentiation was additive.

Conclusion: The present study suggests that aFGF/bFGF/HGF/type IV collagen coating is the efficient condition for hepatic differentiation of UE7T-13 cells, and that WISP1 and WISP2 play an important role in hepatic transdifferentiation of these cells.

Key words: bone marrow, CCN family, hepatocytes, mesenchymal stem cells, transdifferentiation

INTRODUCTION

BONE MARROW IS a reservoir of various stem cells, including hematopoietic stem cells (HSC) and mesenchymal stem cells (MSC). Bone marrow cells have great potential as therapeutic agents, as they are easy to isolate and can be expanded from patients without serious ethical and technical problems. In addition, the use of autologous transplantation of bone marrow-derived cells can prevent immune rejection. Thus, bone marrow-derived cells have several advantages for the development of regenerative medicine.

It has long been thought that the differentiation potential of adult stem cells is limited to their germ layer of origin, but recent studies have demonstrated that adult stem cells are more plastic than once believed.[1–3] Bone marrow cells have been reported to differentiate into hepatocytes.[2,3] The frequency of hepatocytes that were considered to be bone marrow derived varied from 0.5% to 8% in transplanted patients.[1,4,5] *In vivo*

Correspondence: Professor Goshi Shiota, Division of Molecular and Genetic Medicine, Department of Genetic Medicine and Regenerative Therapeutics, Graduate School of Medicine, Tottori University, Tottori, Japan. Email: gshiota@grape.med.tottori-u.ac.jp
Received 15 April 2007; revision 2 May 2007; accepted 3 May 2007.

transplantation studies showed that MSC can differentiate into endodermal cell types as well as having many mesodermal and neuroectodermal characteristics.[6] Bone marrow-derived MSC can differentiate into hepatocytes.[7,8] Hence, human MSC may serve as a source of cell therapy for liver diseases.

An alternative mechanism for plasticity could be the fusion of a bone marrow-derived cell with a non-hematopoietic cell to form a heterokaryon, thereby converting the gene expression pattern of the original bone marrow cell type to that of the fusion partner.[9] However, it remains to be clarified whether cell fusion may generate functionally intact hepatocytes that may not carry a high risk for transformation. In this context, the differentiated hepatocytes from bone marrow cells *in vitro*, which do not mediate cell fusion, are a reliable cell source for regenerative medicine. We therefore attempted to identify the efficient culture conditions and associated genes which regulate hepatic differentiation of human bone marrow-derived cells.

METHODS

Materials

ACIDIC AND BASIC fibroblast growth factor (aFGF, bFGF, respectively) and hepatocyte growth factor (HGF) were obtained from PeproTech EC (London, UK). Oncostatin M (OSM) and leukemia inhibitory factor (LIF) were purchased from DIACLONE Research (Cedex, France) and Alomone Labs (Jerusalem, Israel), respectively. Dexamethasone (Dex) and 5-azacytidine (5-aza) were obtained from Nacalai Tesque (Kyoto, Japan). ITS$^+$ premix (6.25 μg/mL insulin, 6.25 μg/mL transferrin, 6.25 ng/mL selenious acid, 1.25 mg/mL bovine serum albumin, 5.35 mg/mL linoleic acid) and type IV collagen were obtained from Becton Dickinson (Franklin Lakes, NJ, USA).

In vitro hepatic differentiation

Human bone marrow-derived mesenchymal stem cells (hMSC), the life span of which was prolonged by infecting retrovirus encoding human papillomavirus E7 and human telomerase reverse transcriptase (hTERT), designated UE7T-13 cells,[10,11] were used in the present study. To induce hepatic differentiation of UE7T-13 cells, the combined effects of cytokines, 5-aza and type IV collagen coating were examined. First, the effects of cytokines (20 ng/mL aFGF, 10 ng/mL bFGF, 20 ng/mL HGF, 20 ng/mL OSM, 10 ng/mL LIF, 0.5 μM Dex, 50 mg/mL ITS) with or without 10 μM 5-aza treatment were examined.[12–14] UE7T-13 cells were plated on 6-well plates (BD Falcon, Tokyo, Japan) at 9.0×10^3 cells/cm^2 (Fig. 1a). At 6 days, the cells were exposed to 10 μM 5-aza for 24 h. At 7 days, UE7T-13 cells were cultured for 3 weeks in Dulbecco's modified Eagle's medium (DMEM; IWAKI, Tokyo, Japan) containing 10% fetal bovine serum (FBS) and cytokines. Medium changes were performed twice a week, and the cells were replated at 9.0×10^3 cells/cm^2 every week. Second, the combined effects of cytokines, 5-aza and type IV collagen coating on hepatic differentiation were examined with the same schedule (Fig. 1a). Hepatogenesis was assessed by reverse transcription-polymerase chain reaction (RT-PCR) for hepatocyte-specific genes, periodic acid–Schiff staining, albumin staining and urea assay.

Total RNA isolation and real-time RT-PCR

Total RNA was extracted from UE7T-13 cells at 0, 1, 2, 3 and 4 weeks after starting culture using RNAgents Total RNA Isolation System (Promega, Madison, WI, USA). After treatment with DNase (Nippongene, Toyama, Japan), the mRNA was reverse transcribed to cDNA using SuperScript First-Strand Synthesis System for RT-PCR (Invitrogen, Carlsbad, CA, USA).

For RT-PCR, cDNA was amplified using a PCR Thermal Cycler Dice (TaKaRa Bio, Kyoto, Japan) at 94°C for 30 s, the indicated annealing temperature for 30 s, and 72°C for 30 s for 35 cycles. After initial denaturation at 94°C for 5 min, cDNAs of albumin, glutamine synthetase (GS), cytokeratin 18 (CK18), α-fetoprotein (AFP), tyrosine-aminotransferase (TAT), tryptophan 2,3-dioxygenase (TO), glucose-6-phosphatase (G6P), cytochrome p4502B6 (CYP2B6), hepatic nuclear factor 4 (HNF4), c-mpl, c-met, c-kit, LIF receptor, FGF receptor 1, OSM receptor β and glyceraldehyde-3-phosphate dehydrogenase (GAPDH) were amplified using the primers (Table 1). The intensity of the bands was measured by ImageJ (http://rsb.info.nih.gov/ij/). After being normalized by GAPDH, the intensity was expressed as a ratio of expression level at 0 day.

Real-time RT-PCR was done using cDNA and SYBR Green I (Roche, Basel, Switzerland) in a LightCycler 1.5 (Roche Diagnostics, Osaka, Japan). The condition of quantitative RT-PCR was an initial incubation at 95°C for 10 min, followed by 45 cycles at 95°C for 0 s, the indicated annealing temperature for 5 s, and 72°C for product size/25 s. The primers are listed in Table 2. The authenticity and size of the PCR products were confirmed by using a melting curve analysis by LightCycler Software Version 3.5 (Roche Diagnostics) and a gel

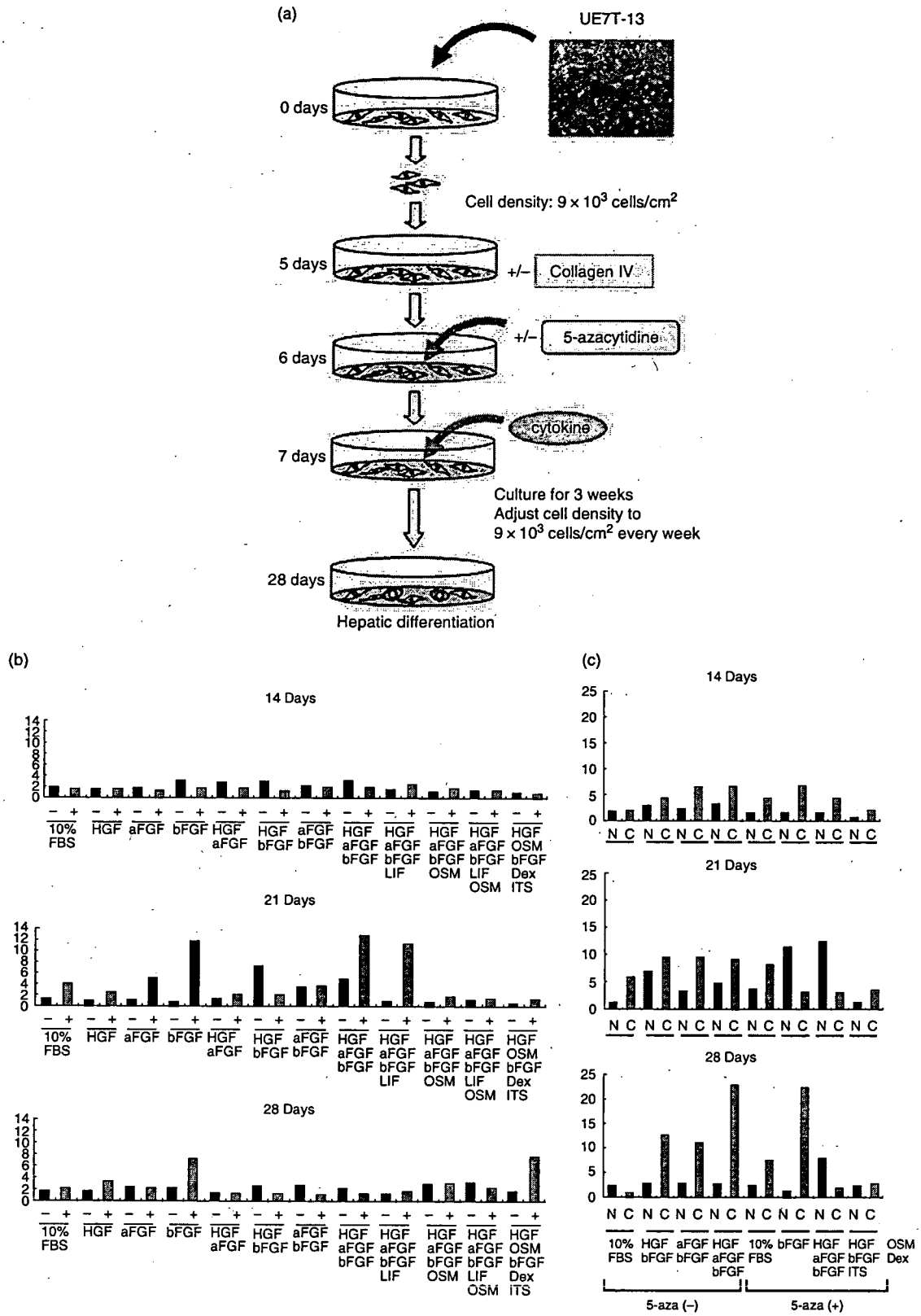

Table 1 Primers for reverse transcription–polymerase chain reaction

		Size (bp)	Temp. (°C)
Albumin	Forward TTGGAAAAATCCCACTGCAT	350	58
	Reverse CTCCAAGCTGCTCAAAAAGC		
GS	Forward GTCAAGATTGCGGGGACTAA	397	58
	Reverse TACGATTGGCTACACCACCA		
CK 18	Forward GAGATCGAGGCTCTCAAGGA	357	58
	Reverse CAAGCTGGCCTTCAGATTTC		
AFP	Forward TGCCAACTCAGTGAGGACAA	356	58
	Reverse TCCAACAGGCCTGAGAAATC		
TAT	Forward TGAGCAGTCTGTCCACTGCCT	358	56
	Reverse ATGTGAATGAGGAGGATCTGAG		
TO	Forward ATACAGAGACTTCAGGGAGC	299	54
	Reverse TGGTTGGGTTCATCTTCGGTATC		
G6P	Forward GCTGGAGTCCTGTCAGGCATTGC	350	56
	Reverse TAGAGCTGAGGCGGAATGGGAG		
CYP2B6	Forward GACGCTACGTTTCAGTCTTTC	204	54
	Reverse GCTGAATACCACGCCATAG		
HNF4	Forward CCAAGTACATCCCAGCTTTC	295	56
	Reverse TTGGCATCTGGGTCAAAG		
c-mpl	Forward TGGAGATGCAGTGGCACTTG	204	57
	Reverse GAGAACTGTGGGGTCTGTAGT		
c-met	Forward ACTCCCCCTGAAAACCAAAGCC	536	60
	Reverse GGCTTACACTTCGGGCACTTAC		
c-kit	Forward TGTGATGATTCTGACCTACA	447	48
	Reverse GAATCACGTTTTCTTCTCAA		
LIFR	Forward GAAAACTGTAAAGCATTACA	504	46
	Reverse AGAGTCTGGAGACACTAA		
FGFR1	Forward CGCTCTAGAGCAGAACTGGGATGTGGGGCTG	832	60
	Reverse CTCGGATCCAGGGCTTCCAGAACGGTC		
OSMRβ	Forward GTGTGGGTGCTTCTCCTGCTTCTGTA	235	56
	Reverse TCTGTGCTAATGACTGTGCTTGTGGT		
GAPDH	Forward GTCTTCTCCACCATGGAGAAGGCT	395	60
	Reverse CATGCCAGTGAGCTTCCCGTTCA		

analysis. mRNA level was normalized using β-actin as an internal control.

DNA microarrays and transfection of siRNA

RNA was extracted from the UE7T-13 cells that were cultured in DMEM containing 10% FBS, 20 ng/mL HGF, 20 ng/mL aFGF and 10 ng/mL bFGF on a type IV collagen dish for 7 days and those that were cultured in 10% FBS on a non-coated dish for 7 days. DNA microarray was performed by using the pathway-specific microarray using Oligo GEArray Human Signal Transduction PathwayFinder™ M (SuperArray Bioscience,

Figure 1 Culture schedule and albumin mRNA expression levels. (a) Induction schedule for hepatic differentiation. UE7T-13 cells were plated at 9×10^3 cells/cm^2 for 5 days. After treatment with or without 5-aza for 24 h, the cells were cultured in the medium containing several kinds of cytokines for 3 weeks. The cells were replated at 9×10^3/cm^2 every week. (b) Expression levels of albumin mRNA at 14, 21 and 28 days in 24 different conditions. Levels of albumin mRNA were expressed as the ratio to GAPDH mRNA. (c) Expression levels of albumin mRNA at 14, 21 and 28 days in 16 different conditions. Levels of albumin mRNA were expressed as the ratio to GAPDH mRNA. aFGF, acidic fibroblast growth factor; bFGF, basic fibroblast growth factor; C, type IV collagen coating; d, days; Dex, dexamethasone; HGF, hepatocyte growth factor; LIF, leukemia inhibitory factor; N, non-coating; OSM, oncostatin M.

Table 2 Primers of real-time reverse transcription–polymerase chain reaction for *CCN* family genes

Gene	Sequences	Size (bp)	Temp.† (°C)
CCN1	Forward CCGAGGTGGAGTTGACGAGAAA Reverse TCTTTCACAAGGCGGCACTCAG	226	65
CCN2	Forward CACCAGCATGAAGACATACCG Reverse CGTCAGGGCACTTGAACTCCA	110	62
CCN3	Forward GGTGCCTGGAGAGTGCTGTG Reverse GGCCTGTAAGCTGCAAGGGTAA	87	64
CCN4	Forward GGAGGCTGCCATCTGTGACC Reverse CACACACTCCTATTGCGTACCTCG	83	60
CCN5	Forward AGTTTTCTGGCCTTGTCTCT Reverse AGAAGCGGTTCTGGTTGGAC	129	62
CCN6	Forward AGTGTGTGCATACCTTGTAGCTG Reverse GGGTTGGGCTGAAACACTTGG	81	65
β-Actin	Forward CGTACAGGTCTTTGCGGATGTC Reverse CACTCTTCCAGCCTTCCTTCC	103	56

†Annealing temperature.

Frederick, MD, USA), which profiles 113 genes representative of 18 signal transduction pathways, according to the manufacturer's instruction. Briefly, cRNA was prepared from cDNA which was reverse transcribed from RNA by a TrueLabeling-AMP Linear RNA Amplification Kit and purified. Hybridization was done overnight using a membrane (Signal Transduction PathwayFinder Oligo GEArray in HybTube Format; Cosmo Bio, Tokyo, Japan). Chemifluorescence was detected by Luminescent Image Analyzer LAS-1000plus (Fujifilm, Tokyo, Japan) and GEArray Expression Analysis Suite (SuperArray Bioscience).

siRNA transfection experiments were performed with double stranded RNAs which were purchased from Hokkaido System Science (Sapporo, Japan). WISP1-specific siRNA-1 and -2 sense-orientation strands with the following sequences (5′-GCCAGGUCCUAUGGA UUAAdTdT-3′) and 5′-CUCGGAUCUCCAAUGUUAAd TdT-3′) were selected. WISP2-specific siRNA-1 and -2 sense-orientation strands with the following sequences (5′-GGUGCGUACCCAGCUGUGCCCGACAdAdG-3′) and (5′-GACCCACCUCCUGGCCUUCUCCCUCdAdG-3′) were also selected. A non-silencing control siRNA (control siRNA Alexa Fluor 488; Invitrogen KK Japan, Tokyo, Japan) sense-orientation strand with the following sequence (5′- UUCUCCGAACGUGUCACGUdTdT-3′) was used. Then, 9×10^3 cells/cm^2 in 24-well plates (BD Falcon) were transfected with RNAiFect Tranfection Reagent (Qiagen) using 1 μg siRNA according to the manufacturer's instruction. Transfection efficiency in cells was determined with fluorescein isothiocyanate (FITC)-labeled siRNA (control siRNA Alexa Fluor 488) and evaluated by cell counting using a fluorescent microscope (Olympus IX71; Olympus, Tokyo, Japan) to be 90–95% after 24 and 48 h. To examine the effect of siRNA on cell differentiation, WISP1-specific siRNA2 and WISP2-specific siRNA2 were transfected with UE7T-13 cells weekly up to 4 weeks after starting cell culture.

Immunocytochemistry, periodic acid–Schiff stain for glycogen

Cells were fixed overnight with 4% formaldehyde at 4°C, and permeabilized with 0.1% Triton X-100 (Wako Pure Chemical Industries, Osaka, Japan) for 10 min. Slides were incubated with mouse primary antibody against human albumin (1:1000) (Sigma-Aldrich, St Louis, MO, USA) at 37°C for 1 h, and then stained with the avidin–biotin–peroxidase complex (Vector Laboratories, Burlingame, CA, USA).

Culture dishes were fixed in 4% formaldehyde, permeabilized with 0.1% Triton X-100 for 10 min and either were not incubated or were incubated with α-amylase (Nacalai Tesque) for 3 h at 37°C. Samples were then oxidized in 1% periodic acid for 5 min, rinsed three times in deionized (d) H_2O treated with Schiff's reagent (Nacalai Tesque) for 15 min, and rinsed in dH_2O three times. Samples were counterstained with Mayer's hematoxylin for 1 min and assessed under a light microscope (Olympus BX41; Olympus). The percentages of albumin-positive or periodic acid–Schiff (PAS)-positive cells were expressed as the number of positive cells divided by the total cell number of eight randomly selected fields.

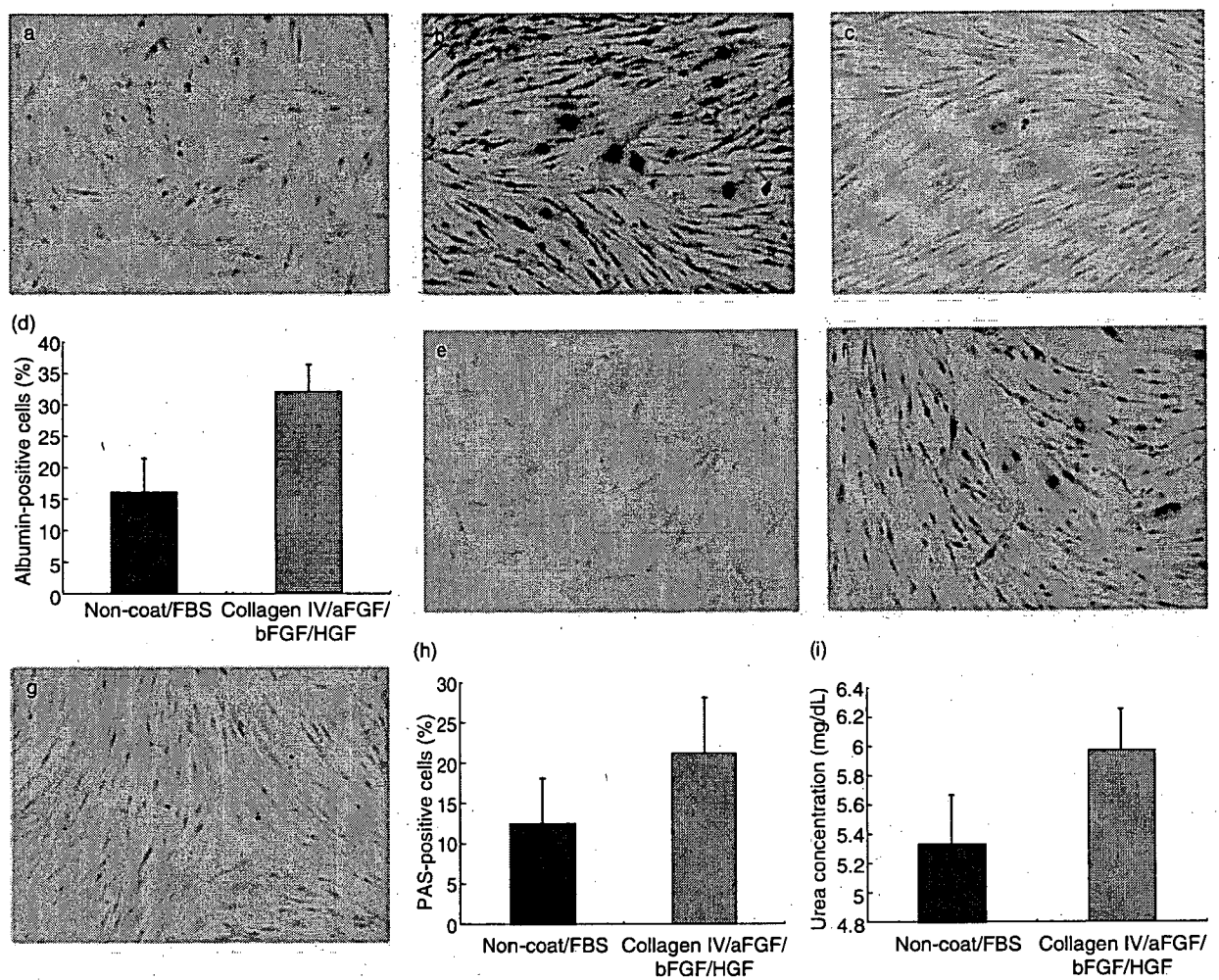

Figure 2 Functional assays of hepatocyte-like cells. (a) UE7T-13 cells (albumin staining, original magnification ×200). (b) UE7T-13 cells cultured in HGF/aFGF/bFGF on type IV collagen-coated dish for 21 days (albumin staining, original magnification ×200). Hepatocyte-like cells which express much albumin appear. (c) UE7T-13 cells cultured in 10% fetal bovine serum (FBS) on non-coated dish for 21 days (albumin staining, original magnification ×200). (d) Percentages of albumin-positive cells cultured in HGF/aFGF/bFGF on type IV collagen-coated dish and 10% FBS on non-coated dish. Data are expressed as mean ± SD of five experiments. (e) UE7T-13 cells (periodic acid–Schiff [PAS] staining, original magnification ×200). (f) UE7T-13 cells cultured in HGF/aFGF/bFGF on type IV collagen-coated dish for 21 days (PAS staining, original magnification ×200). Hepatocyte-like cells which store glycogen appear. (g) UE7T-13 cells cultured in 10% FBS on non-coated dish for 21 days (PAS staining, original magnification ×200). (h) Percentages of PAS staining-positive cells cultured in HGF/aFGF/bFGF on type IV collagen-coated dish and 10% FBS on non-coated dish. Data are expressed as mean ± SD of five experiments. (i) Urea production in the media of the cells cultured in HGF/aFGF/bFGF on type IV collagen-coated dish and 10% FBS on non-coated dish. Data are expressed as mean ± SD of five experiments. aFGF, acidic fibroblast growth factor; bFGF, basic fibroblast growth factor; HGF, hepatocyte growth factor.

Urea assay

UE7T-13 cells in 24-well plates (BD Falcon) were cultured in 5 mM ammonium chloride (Nacalai Tesque) for 48 h, and then urea concentrations were determined by QuantiChrom Urea Assay Kit (BioAssay Systems, Hayward, CA, USA) according to the manufacturer's instruction, and were analyzed with HITACHI U-1500 (Hitachi, Tokyo, Japan). The data were expressed as mean ± SD of five experiments.

RESULTS

Optimal conditions for hepatic differentiation

UE7T-13 CELLS, which originally have the ability of osteogenic, chondrogenic, and adiopogenic differentiation, can be differentiated into cardiomyocytes and neurons;[12,15] however, hepatic differentiation ability has been unknown. UE7T-13 cells strongly express c-kit, c-met, FGF receptor 1, and OSM receptor, but weakly express LIF receptor β (data not shown). To determine the optimal method of hepatic differentiation, the first experiments were done in 24 culture conditions using HGF, aFGF, bFGF, LIF, OSM, Dex, ITS and 5-aza (Fig. 1b). UE7T-13 cells scarcely express albumin mRNA at 0 day. In the absence of 5-aza, higher expression of albumin mRNA was observed in the conditions of HGF/bFGF, aFGF/bFGF and HGF/aFGF/bFGF at 21 days; however, expression level decreased at 28 days. In the presence of 5-aza, albumin mRNA was strongly expressed in culture conditions of aFGF, bFGF, HGF/aFGF/bFGF and HGF/aFGF/bFGF/LIF at 21 days, and was still higher in bFGF and HGF/OSM/bFGF/Dex/ITS at 28 days. Overall expression of albumin mRNA was decreased at 28 days (Fig. 1b). Then, the cells were examined for hepatogenesis on type IV collagen as scaffold protein, because a type IV collagen coating stimulated colony formation of mouse hepatic progenitor cells.[16] The combined effects of cytokines, 5-aza and type IV collagen were examined in 16 types of culture conditions (Fig. 1c). In the presence of type IV collagen, the cells expressed a higher level of albumin mRNA; however, in the absence of type IV collagen they did not. At 28 days, the highest expression of albumin mRNA was obtained in the cells cultured in the condition of HGF/aFGF/bFGF/collagen coating, and higher expression was observed in the condition of bFGF/5-aza/collagen coating.

By RT-PCR analysis, expression of other hepatocyte-specific genes such as *AFP*, *K-18*, *G6P*, *TAT*, GS and *TO* was examined at 28 days. Expression of these genes tended to be higher in 5-aza-treated cells, especially in the cells treated with bFGF/5-aza/collagen coating, and was also higher in the condition of HGF/aFGF/bFGF/collagen coating. Expression of CYP2B6 and HNF4 was not observed until 4 weeks after induction (data not shown).

Table 3 DNA microarray analysis.

Symbol	Pathway	Group 1/Group 2
Upregulated genes		
BCL2A1	Survival (NF-κB)	2.970779996
CCL20	NF-κB	1.978631867
FOXA2	Hedgehog	1.504629504
GREB1	Estrogen	1.505453786
IL1A	NF-κB	1.827547367
IL4	Jak-Stat	1.752106063
NOS2A	Jak-Stat	1.536994317
LEP	Insulin	1.944428028
PECAM1	NF-κB	1.576490344
PGR	Estrogen	1.581404729
PTGS2	Phospholipase C	5.000349291
RBP1	Retinoic acid	1.646096039
SELE	LDL	2.16645166
TMEPAI	Androgen	1.953435518
TRIM25	Estrogen	4.422090754
VEGF	Wnt	2.308966453
WSB1	Hedgehog	1.695788997
Downregulated genes		
ATF2	Stress	0.535377059
BAX	p53	0.516648555
BCL2	Estrogen	0.579983284
BIRC1	Survival (NF-κB)	0.553646131
BIRC2	Survival (NF-κB)	0.645158295
BIRC5	Wnt	0.505786989
BMP4	Hedgehog	0.585645362
BRCA1	Estrogen	0.585153761
CD5	NFAT	0.621715546
CDK2	Androgen	0.565415139
CDKN1C	TGF-beta	0.557206377
CDKN2A	TGF-beta	0.50807409
CDKN2B	TGF-beta	0.480227082
CDX1	Retinoic acid	0.547114338
C/EBPβ	Insulin	0.600885902
CSN2	Jak-Stat	0.562621027
CTSD	Estrogen	0.491377292
CXCL12	Estrogen	0.215851667
EN1	Hedgehog	0.499769336
HK2	Insulin	0.62796643
HSPCA	Stress	0.572358328
IGFBP3	p53	0.501512431
IKBKB	NF-κB	0.419132357
TANK	NF-κB	0.631916221
FAS	p53	0.593650284
FASLG	NFAT	0.262290028
TP53	p53	0.128023898
WISP1	Wnt	0.212766767
WISP2	Wnt	0.102305807

LDL, low-density lipoprotein; NF-κB, nuclear factor kappa B; TGF, tumor growth factor.

Immunocytochemistry of the differentiated cells

While undifferentiated UE7T-13 cells did not express albumin (Fig. 2a), Four-week-culture condition of HGF/aFGF/bFGF/collagen coating induced many albumin-positive cells (Fig. 2b). Some round or oval-shaped cells appeared in fibroblastic bipolar MSC, and these cells began to lose their edges and progressed toward the polygonal morphology of hepatocytes in a time-dependent manner. The culture condition of 10% FBS/non-coating induced far fewer hepatocyte-like cells (Fig. 2c). The rate of albumin positivity was 32% by HGF/aFGF/bFGF/collagen coating, whereas only 15% of cells were positive for albumin in 10% FBS/non-coated culture (Fig. 2d). The presence of glycogen in many cells, which were examined by PAS staining, was accelerated by HGF/aFGF/bFGF/collagen coating, while not as many cells were stained by 10% FBS/non-coating (Fig. 2e–h). When pretreated with α-amylase to digest glycogen, the cells were negative for glycogen (data not shown). Interestingly, binuclear cells, which are a typical feature of hepatocytes, appeared (Fig. 2f). In addition, HGF/aFGF/bFGF/collagen-coated cells synthesize significantly higher amounts of urea than 10% FBS/non-coated cells (Fig. 2i).

Genes which are associated with hepatic differentiation

To identify the genes which are induced by optimal condition, a pathway-specific microarray was performed. Of 113 genes, 17 genes were upregulated and 30 genes were downregulated (Table 3). Of these genes, expression of *WISP1* (Wnt-1 induced secreted protein 1, CCN4) and *WISP2* (Wnt-1 induced secreted protein 2, CCN5) genes was reduced to 21% and 10% of the control condition, respectively. Wnt signal regulates self-renewability of hematopoietic stem cells[11] and CCN family proteins are associated with cell growth and differentiation.[17] Indeed, it has been reported that *WISP1* is an osteoblastic regulator during skeletal development[18] and CCN1 plays an important role in osteoblast differentiation.[16] Expression of *WISP1* was greatly reduced in HGF/aFGF/bFGF/

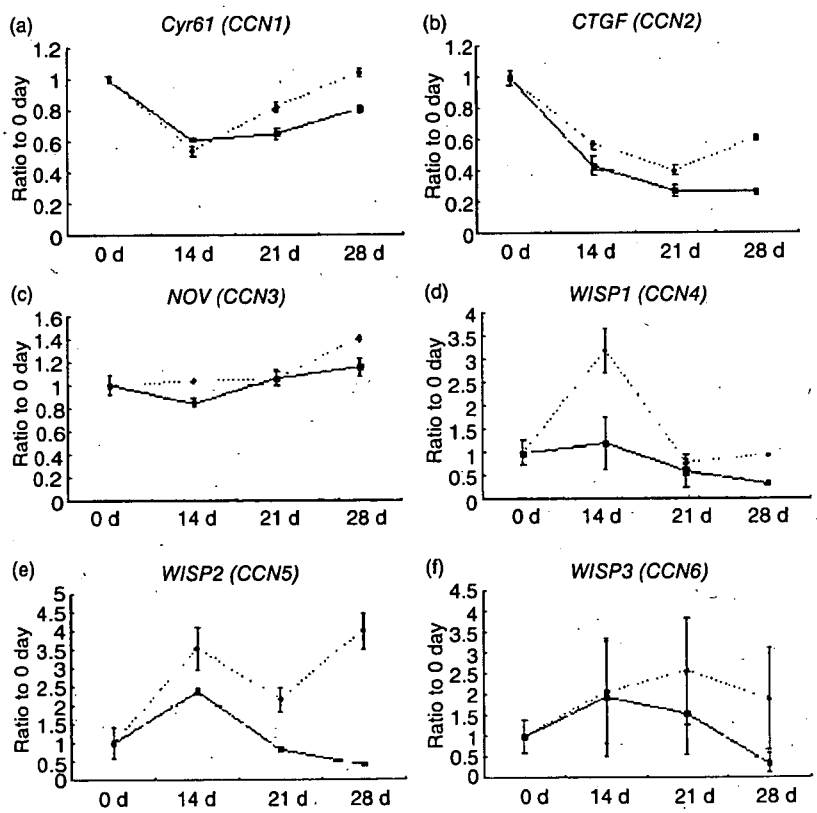

Figure 3 Serial analysis of CCN family mRNA expression. (a) *Cyr61* (*CCN1*). Data are expressed as mean ± SD of five experiments. (b) *CTGF* (*CCN2*). (c) *NOV* (*CCN3*). (d) *WISP1* (*CCN4*). (e) *WISP2* (*CCN5*). (f) *WISP3* (*CCN6*). (·····), Control; (——), HGF/aFGF/bFGF/collagen coating.

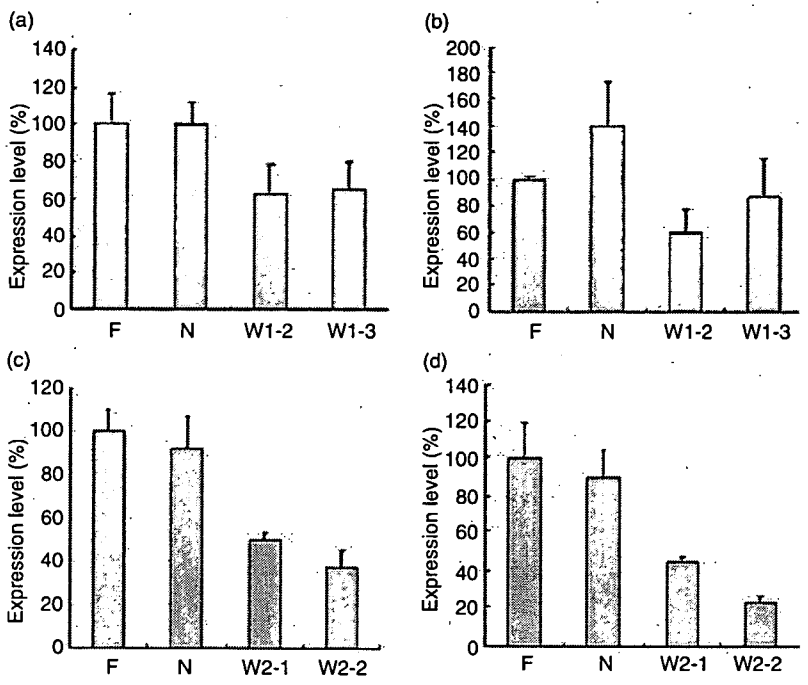

Figure 4 Expression level of WISP1 and WISP2 mRNA at 24 and 48 h after siRNA transfection. (a) Expression of WISP1 mRNA at 24 h after transfection. siRNAs include three types of WISP1-siRNA and two types of WISP2-siRNA. F, 10% fetal bovine serum (FBS) only; N, non-silencing control siRNA; W1-2, WISP1-siRNA no. 2; W1-3, WISP1-siRNA no. 3. Data are expressed as mean ± SD of five experiments. (b) Expression of WISP1 mRNA at 48 h after transfection. (c) Expression of WISP2 mRNA at 24 h after transfection. F, 10% FBS only; N, non-silencing control siRNA; W2-1, WISP2-siRNA no. 1; W2-2, WISP1-siRNA no. 2. (d) Expression of WISP2 mRNA at 48 h after transfection.

collagen-coated cells at 14 days, and was still lower at 28 days although the difference was small (Fig. 3d). Reduced expression of *WISP2* was observed at 14, 21 and 28 days (Fig. 3e). Expression of CCN1, 2, 3 and 6 was not changed by the condition of HGF/aFGF/bFGF/collagen coating (Fig. 3a–c,f).

Knockdown of *WISP1* and *WISP2*

By siRNA transfection of W1-2, expression of *WISP1* was reduced to about 60% and after 24 and 48 h (Fig. 4a,b), respectively. W1-3 transfection caused reduction of *WISP2* mRNA to 63% after 24 h and 88% after 48 h (Fig. 4a,b). Expression of *WISP2* by W2-1 was decreased to 50% and 45% after 24 and 48 h, respectively (Fig. 4c,d). W2-2 reduced *WISP2* mRNA to 38% at 24 h and to 22% at 48 h (Fig. 4c,d). The culture condition of HGF/aFGF/bFGF/collagen coating reduced *WISP1* mRNA and *WISP2* mRNA (Fig. 5a,b). siRNA specific for *WISP1* decreased expression of WISP1 mRNA in the cells of both 10% FBS/non-coat and HGF/aFGF/bFGF/collagen coating (Fig. 5a). siRNA specific for WISP2 also inhibited expression of WISP2 mRNA in both 10% FBS/non-coating and HGF/aFGF/bFGF/collagen coating (Fig. 5b). In 10% FBS/non-coated cells, WISP1-siRNA and WISP2-siRNA increased albumin-positive cells ($P < 0.01$ and $P < 0.05$, respectively, Fig. 6c). The effect of WISP2-siRNA and HGF/aFGF/bFGF/collagen-coating condition was additive in increasing albumin-positive cells ($P < 0.01$, Fig. 5c). However, the effect of WISP1-siRNA with HGF/aFGF/bFGF/collagen coating was not different from that with HGF/aFGF/bFGF/collagen coating. The PAS-positive cells were increased by WISP1-siRNA and WISP2-siRNA, compared with control siRNA ($P < 0.01$, each, Fig. 5d). Transfection with WISP2-siRNA in combination with HGF/aFGF/bFGF/collagen-coated condition increased the PAS-positive cells, compared with HGF/aFGF/bFGF/collagen-coated condition ($P < 0.01$); however, WISP1-siRNA did not. Transfection with WISP1-siRNA or WISP2-siRNA induced greater urea production ($P < 0.01$, each, Fig. 5e), and the bigger effect was observed in combination of HGF/aFGF/bFGF/collagen coating with WISP1-siRNA or WISP2-siRNA ($P < 0.01$, each).

The effects of WISP1-siRNA and WISP2-siRNA on changes of morphology were evident; the cells became extended, round and oval-shaped cells by WISP1-siRNA/non-coat (Fig. 6a), and the cell shape became more extended by WISP2-siRNA (Fig. 6b), while many cells remained fibroblastic shaped in 10% FBS/non-coated condition (Fig. 6c). Combination of WISP1-siRNA with HGF/aFGF/bFGF/collagen-coated condition promoted hepatic morphogenesis (Fig. 6d). Albumin

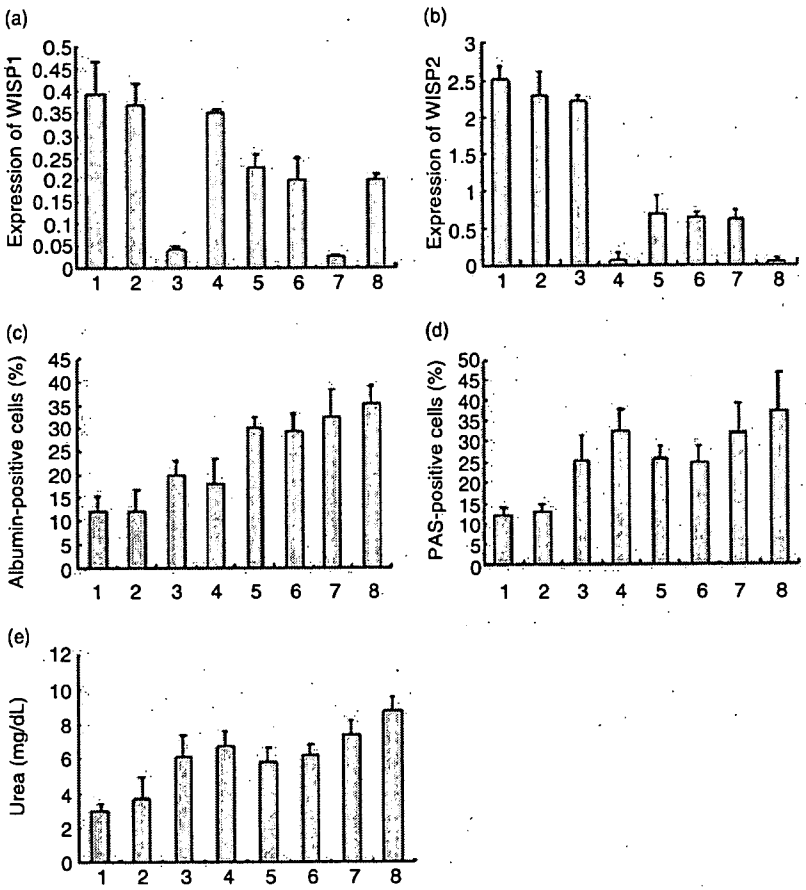

Figure 5 Effects of knockdown of WISP1 and WISP2 on hepatic differentiation. (a) Expression level of WISP1 mRNA at 28 days after weekly transfection of WISP1-siRNA.1, 2, 3 and 4 represent the condition of 10% fetal bovine serum (FBS)/non-coat, and 5, 6, 7 and 8 represent the condition of HGF/aFGF/bFGF/collagen coating. 1 and 5, no transfection; 2 and 6, transfection with non-silencing control siRNA; 3 and 7, transfection with WISP1-siRNA; no. 2; 4 and 8, transfection with WISP2-siRNA no. 2. Data are expressed as mean ± SD of five experiments. (b) Expression level of WISP2 mRNA at 28 days after weekly transfection of WISP2-siRNA. (c) Percentages of albumin-positive cells. (d) Percentages of periodic acid–Schiff (PAS)-positive cells. (e) Urea production in the media.

was more densely stained in these cells. PAS staining showed that WISP2-siRNA combined with HGF/aFGF/bFGF/collagen coating induced much glycogen deposition in hepatocyte-like cells (Fig. 6e), whereas glycogen-stored cells were much fewer in the cells of 10% FBS/non-coated condition (Fig. 6f).

DISCUSSION

IN THE PRESENT study, we examined two steps to study the conditions to induce hepatic differentiation. First, the effect of combination of cytokines and 5-aza on hepatic differentiation was studied. 5-aza was used because cardiomyogenic differentiation of murine bone marrow stromal cells was approximately 30% by 5-aza.[14] Treatment with 5-aza and bFGF actually caused hepatic differentiation, judging from expression of albumin as well as other liver-specific genes. Hence, demethylation of genes may be important for differentiation of MSC. The cytokines whose receptors were expressed were used (data not shown). During embryonic development, the production of growth factors such as HGF and FGF has been associated with endoderm specification.[19,20] In addition, HGF may be an important regulator in the early stage of hepatogenesis, as HGF plays a role in regeneration of acute hepatitis.[21] Second, the combined effects of cytokines and type IV collagen coating were examined, because type IV collagen was the most potent inducer of colonization of hepatic progenitor cells.[10] The importance of the extracellular matrix in the liver developmental process has increasingly been recognized.[22] Undifferentiated mouse ES cells express integrins α6, β1, β4, β5, laminin receptor 1 and dytroglycan, and are thus poised to receive signals from the extracellular matrix.[23] Mouse hepatic progenitor cells in fetal liver express CD49f (α6 inetgrin) and CD29 (β1 integrin), and these cells respond well to type IV collagen.[10] E7T-13 cells were reported to express CD29 and CD49,[12] and these molecules may be important for hepatic differentiation.

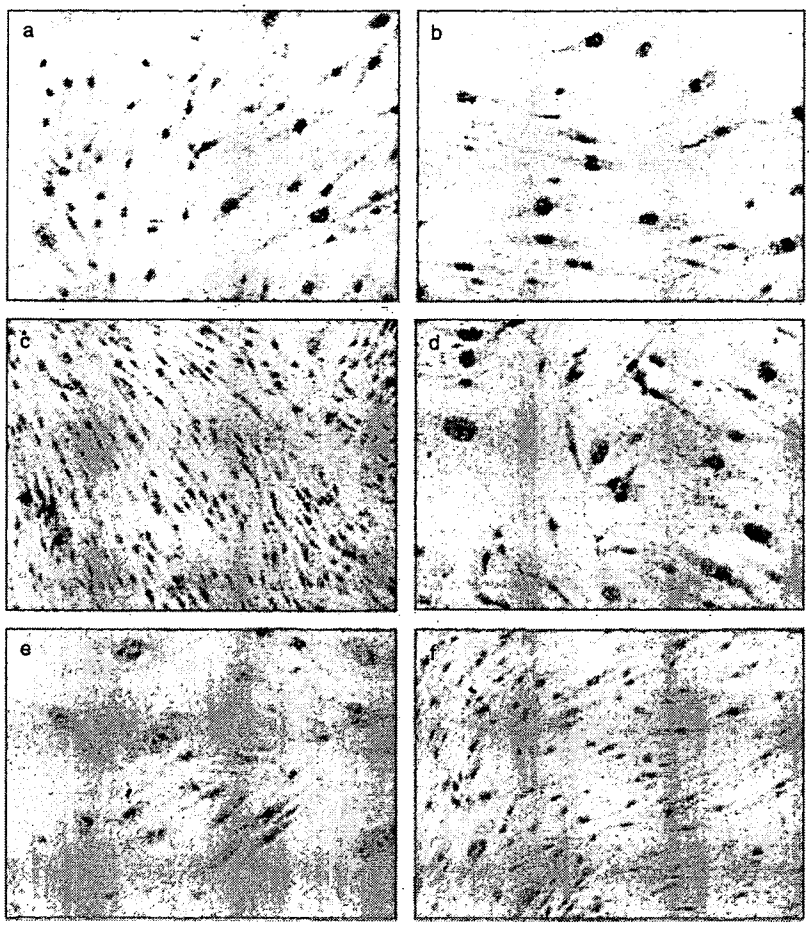

Figure 6 Cytochemical analysis of the cells. (a) UE7T-13 cells cultured in 10% fetal bovine serum (FBS)/non-coated condition with transfection of WISP1-siRNA (albumin staining, original magnification ×200). (b) UE7T-13 cells cultured in 10% FBS/non-coated condition with transfection of WISP2-siRNA (albumin staining, original magnification ×200). (c) UE7T-13 cells cultured in 10% FBS/non-coated condition with transfection of non-silencing control siRNA (albumin staining, original magnification ×200). (d) UE7T-13 cells cultured in HGF/aFGF/bFGF/collagen-coated condition with transfection of WISP1-siRNA (albumin staining, original magnification ×200). (e) UE7T-13 cells cultured in HGF/aFGF/bFGF/collagen-coated condition with transfection of WISP2-siRNA (periodic acid–Schiff [PAS] staining, original magnification ×200). (f) UE7T-13 cells cultured in 10% FBS/non-coated condition with transfection of non-silencing control siRNA (PAS staining, original magnification ×200).

In the present study, downregulation of *WISP1* and *WISP2* during hepatic differentiation was observed. Knockdown experiments of these genes confirmed the critical roles of these genes in hepatic differentiation of MSC. *WISP1* and *WISP2* belong to the CCN family, which are involved in the control of cell proliferation and differentiation by participating in internal and external cell signaling.[17] The CCN family include *CYR61* (*CCN1*), *CTGF* (*CCN2*), *NOV* (*CCN3*), and *ISP*-1 (*CCN4*), *WISP*-2 (*CCN5*) and *WISP*-3 (*CCN6*). *WISP1* and *WISP2* are downstream in the WNT1/β-catenin signaling pathway. *WISP2* was identified as a regulator of osteoblast function.[24] Interestingly, differential expression of CCN family genes in bone marrow-derived MSC during osteogenic, chondrogenic and adipogenic differentiation was observed.[25] *WISP2* expression declined during adipogenic differentiation, and *WISP3* expression was markedly reduced in chondrogenic differentiation. In addition, both WISP1 and CCN1 were reported to be an osteoblastic regulator of MSC during skeletal development and fracture repair.[16,18] These reports suggest that the CCN family proteins are important regulators of differentiation of MSC. MRP-1/CD9, which downregulates several *Wnt* family genes including *WISP1*, *WISP3* and *c-myc*, has been reported to suppress cell transformation including epithelial to mesenchymal transition through downregulation of Wnt.[26] In this context, one possible mechanism responsible for hepatic differentiation of MSC by WISP1 and WISP2 may be associated with mesenchymal epithelial transition.

Human bone marrow MSC are easy to isolate but difficult to study because of their limited life span. The advantages of using UE7T-13 cells in the repopulation study are as follows; the cells have the same expression pattern of surface markers with parental H4-1 cells,